Sublimation from Sharp-edged Cylinders in Axisymmetric Flow, Including Influence of Surface Curvature

WILLIAM J. CHRISTIAN and STOTHE P. KEZIOS

Illinois Institute of Technology, Chicago, Illinois

An experimental investigation was performed on the mass transfer by sublimation from the outer surfaces of hollow naphthalene cylinders, 0.75 and 1.00 in. in diam., in parallel air streams at velocities between 20 and 120 ft./sec. Local mass transfer rates on the cylinders were obtained by a profilometric technique consisting of accurate determinations of changes in radii of the subliming surfaces at points along elements of the cylinders.

Local coefficients of mass transfer obtained with laminar boundary layers for Reynolds numbers (based on axial length) between 12,000 and 100,000 were found to be up to 8% greater, because of surface curvature, than corresponding values for flat surfaces. Moreover comparison of the mass-transfer data with a theoretical prediction for laminar skin friction on circular cylinders indicates an effect of surface curvature on the Chilton-Colburn anology between momentum and mass transfer amounting to as much as 6% in the range of air velocity employed. For turbulent boundary layers obtained by artificial triggering of turbulence at the leading edges of the cylinders no effect of surface curvature was found. The results obtained for Reynolds numbers of 40,000 to 1,000,000 are lower than previously published correlations of turbulent heat, mass, and momentum transfer, when compared by the Boelter, Martinelli, and Jonassen form of the analogy.

Theoretical and semiempirical studies dealing with the influence of transverse curvature on axially symmetric laminar and turbulent boundary layers have appeared in the literature (*1* through *11*) for the specific case of the circular cylinder. These analyses have been based on an idealized model, with walls of zero thickness, which admits flow through its center without disturbance of the external field at the leading edge. Whereas the results of experimental investigations with cylinders oriented axially with the flow have been published (*2*, *4*, *12* through *15*), experimental information on transport processes (momentum, heat, and mass) for the particular case of the sharp-edged cylinder in axisymmetric flow apparently does not exist.

In this investigation experimental data were obtained for a transport process at the surface of a cylinder which simulates the ideal model. In this connection experiments based on any of the three transport processes usually employed, namely momentum, heat, and mass transfer, are possible. Since there is flow on the inside as well as the outside of such a model, it would be extremely difficult, if at all possible, to determine the skin friction at the outer surface by direct force measurements. Moreover the alternative method of finding the skin friction by probing the boundary layer along the outer surface is unattractive because of unduly delicate instrumentation and fine techniques. Likewise a heat transfer model would present the usual problems of insulation and guard heating, particularly near the sharp leading edge.* Therefore a study based on the mass transfer phenomenon presents the least difficult experimental approach and was used in this work. Several years' work in the Illinois Institute of Technology Heat Transfer Laboratory with sublimation of organic solids, particularly naphthalene, has demonstrated the utility of this technique.

William J. Christian is with the Armour Research Foundation, Chicago, Illinois.

*The leading edge of the hollow cylinder may be likened to the usual conception of the sharp leading edge of a flat plate. In reality the flat plate is a special kind of cylinder for which the radius of curvature is infinitely large.

Table 1—Dimensions of Hollow Sublimation Models in Inches

Dimension	Model 1	Model 2
Outside diameter*	0.998	0.749
Inside diameter	0.625	0.432
Over-all length	26.0	18.2
Active length	20.0	11.3
Starting length	0.127	0.129

*Tolerance: model 1, +0.010, −0.000 in.; model 2, +0.005, −0.000 in.

APPARATUS AND TECHNIQUES

Models

The hollow sublimation models consist of sharp-edged metal tubes over which layers of naphthalene were cast (Figure 1). Table 1 shows the important dimensions of of the two cylinders employed. The sharp leading edge of each cylinder is formed by a 60-deg. conical inlet at the nose. To provide permanent (nonsubliming) leading edges and to maintain finite naphthalene thicknesses at the forward edges of the subliming surfaces, metal sections (hydrodynamic starting sections) about ⅛ in. long were used ahead of the naphthalene on both cylinders. Molds for casting the naphthalene layers on the metal tubes were made from dental plaster by using polished, stainless steel cylinders as master patterns.

A small naphthalene cylinder light enough to weigh on an analytical balance was used to compare the true weight loss by sublimation to the weight loss determined from surface profile measurements. This cylinder is 1 in. in diameter and about 4 in. long with an approximately spherical metal nose.

A hollow cylinder made entirely of metal was used to study pressure distributions for flows over the experimental models. This pressure model simulates the 1 in. sublimation model in all dimensions except its length, which is 12 in. Pressure taps (a total of sixteen) distributed over its exterior consist of $\frac{1}{32}$ in.-diameter holes drilled at right angles to the surface and so located around the cylinder that no tap is immediately downstream of any other.

The models are shown in Figure 2 along with one half of each mold used for casting the naphthalene. From left to right they are: the 1-in. sublimation model, the 1-in. pressure model, the ¾-in. sublimation model, and the hemispherically capped sublimation model.

Flow Facility

The air stream used was produced in an open-circuit, induced-draft wind tunnel shown schematically in Figure 3. Its diameter is 48 in. at the inlet and 12 in. at the throat; the length of the test section is 36 in., and the over-all length of the tunnel is approximately 20 ft. Turbulence-damping screens and the large nozzle-contraction ratio (16 to 1) favor low turbulence in the test region. The velocity of air in the unobstructed test section is constant within 2% in the central 10 in. of the throat over its entire length.

As shown in Figure 3, the tapered socket supporting the models is connected to a short length of pipe which is suspended within the diffuser by six steel wires. Connection is made from this pipe through an orifice flow meter to a vacuum tank for exhausting air through the center of the hollow models. The required vacuum pressures of up to 3 lb./sq. in. were maintained in the tank by a rotary-lobe type of blower.

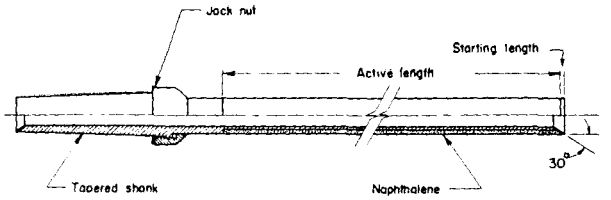

Fig. 1. Details of hollow cylinders.

Surface Profilometer

Material losses and hence sublimation rates for the naphthalene cylinders were obtained from precise measurements of changes in radii at a number of points along the surface. These measurements were made by using a micrometer dial indicator while the cylinders were held between centers of a 42 in.-long lathe bed. The indicator is mounted on the lathe carriage to provide for axial movement along the cylinders; it is graduated in 0.0001 in., and its reading may be estimated within about 0.00002 in. Contact of the indicator with the top surface of the cylinder is made through a $\frac{1}{16}$-in.-diam. tip, the working end of which is rounded to a $\frac{3}{16}$-in. radius. To minimize loss of naphthalene during measurement of the cylinders the apparatus is housed in an enclosure with the atmosphere essentially saturated with naphthalene vapor.* Provision is made for external control of the position of the indicator.

Indicator readings were obtained at a number of stations along each cylinder before and after exposure to the air stream. To minimize marring of the naphthalene, the indicator tip was raised from the surface (by using a solenoid) while positions were changed. Clearly the difference in indicator readings at each station is a direct measure of the local mass transfer. Measurement of the axial position of each station with respect to the leading edge of the cylinder was obtained from the number of revolutions made by the lead screw and its pitch.†

Values of the change in radius of the naphthalene cylinders were obtained for four circumferential positions at each axial station; these values were within 5% of their arithmetic average, which was used in all cases for determining the local mass transfer at each position along the cylinders.

Temperature Measurement

The vapor pressure–temperature relationship for naphthalene, which follows the Clausius-Clapeyron form, requires an accuracy of 0.1°F. in temperature measurement if the vapor pressure is to be known within 1%. This accuracy was sought in this work.

Direct measurement of the surface temperature of the solid, which would be complicated because of the continuous removal of surface material through sublimation, was not employed in this work. Instead only the temperature of the air stream was measured by using a calibrated copper-constantan thermocouple located 3 in. downstream of the subliming surfaces, 1½ in. above the cylinder axis. Surface temperatures of the cylinders were within the required 0.1°F. of the indicated air temperatures, since aerodynamic heating* and surface-temperature depression† due to sublimation were negligible in the range of variables employed.

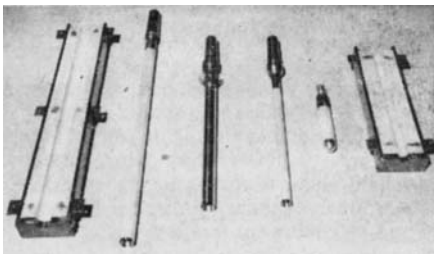

Fig. 2. Experimental models.

Physical Properties

Air densities were calculated according to the ideal-gas law with the usual value of 0.0808 lb./cu. ft. used for the density at standard conditions (32°F., 1 atm.). Values of the kinematic viscosity were taken from a compilation of air properties published by Jakob (*16* and *17*).

In the absence of reliable data on the diffusion coefficient for air and naphthalene vapor, Gilliland's semiempirical correlation (*18*) was employed. Introduction of appropriate constants in Gilliland's equation results in the following relation for air-naphthalene mixtures:

$$\delta = \frac{20.25T^{\frac{3}{2}}}{p} \qquad (1)$$

Here δ is in sq. ft./hr., T in °R., and p in atm.

The specific gravity of solid naphthalene seems to be available at only two temperatures (*19*), 62.6 and 68.0°F. Extrapolation to higher temperatures was carried out on the assumption of a linear temperature dependence, namely

$$\rho_s = 82.42 - 0.1611t \qquad (2)$$

Density is given in pounds per cubic foot by Equation (2) with temperature t in degrees Fahrenheit.

The literature on vapor pressure of solid naphthalene has been reviewed by Kezios (*20*), who also obtained vapor-pressure data for a grade of naphthalene comparable to that used in the present work (Baker's C.P.). His results* and those of others (*21*, *22*) which appear to be mutually consistent have been used here to determine a vapor pressure-temperature relationship. The data are shown in Figure 4 along with the straight line fitted by the method of least squares. The correlating equation is

$$\log_{10} p^* = 12.198 - 6{,}881/T \qquad (3)$$

In Equation (3) vapor pressure is in pounds per square foot, and temperature in degrees Rankine.

FLOW AND PRESSURE DISTRIBUTION

The ideal sharp-edged cylinder which admits air through its center would have uniform pressure over its outer surface, and all stream surfaces would be circular cylinders if the external and internal flows were balanced. But in practice an exact balance of internal and external flow is difficult to maintain because of minor variations in the flow rates. The consequences of unbalance of the flows may be understood if the potential flow near the inlet of an idealized hollow cylinder is considered qualitatively (*23*). Figure 5, showing cross-sectional sketches of the stream surfaces for R_u greater and less than unity, depicts the two conditions of unbalance. Clearly the stagnation of the flow occurs on the inside of the cylinder for $R_u < 1$ and on the outside for $R_u > 1$, whereas it would be expected to occur just at the leading edge for the balanced situation, where R_u is unity. For both $R_u \lesseqgtr 1$, the stagnation stream surface must branch into two separate parts at the stagnation line, and each of these parts must follow the solid boundary, one in the upstream direction the other downstream. Theoretically the branch that moves upstream must turn through 180 deg. at the leading edge to maintain contact with the surface. Since such a sudden turn is not physically possible, the real flow is characterized by a separation at the leading edge with the formation of a burble and the generation of turbulence. Moreover the turbulence will be created on the outer surface for $R_u < 1$ and on the inner surface for $R_u > 1$. It is evident then that a laminar boundary layer can occur on the outside of the cylinder only when $R_u \geq 1$, and if a turbulent boundary layer is to be generated on the outside surface, transition of flow can be promoted by operation with $R_u < 1$.

The present sublimation experiments demonstrated that the models did indeed behave in this manner; accordingly, the nature of the boundary layer was

*In spite of this, small losses during measurement did occur. Loss rates were determined in auxiliary tests and used as a basis for correction of the main sublimation data; the maximum correction encountered was about 2.5%.

†The accuracy of the pitch was found to be 1% or better for all distances from the leading edge greater than 1 in. The screw was calibrated with a dial indicator for distances less than 1 in. from the leading edge to provide 1% accuracy in that region also.

*Though the recovery temperature of the cylinder was as much as 0.8°F. above ambient temperature in some of the experiments, the difference between the recovery (indicated) temperature of the thermocouple and that of the cylinder could not have been more than 0.05°F.

†The surface-temperature depression amounted to slightly more than 0.1°F. at places within about ¾ in. of the leading edge of the cylinder. Correction for this small effect seemed unwarranted, since the mass transfer data for this region were uncertain for other reasons, for instance the approximate correction used to account for the effect of the metal starting section.

*Kezios's data for temperatures above about 85°F. are probably somewhat high, as he himself indicated, and were disregarded here.

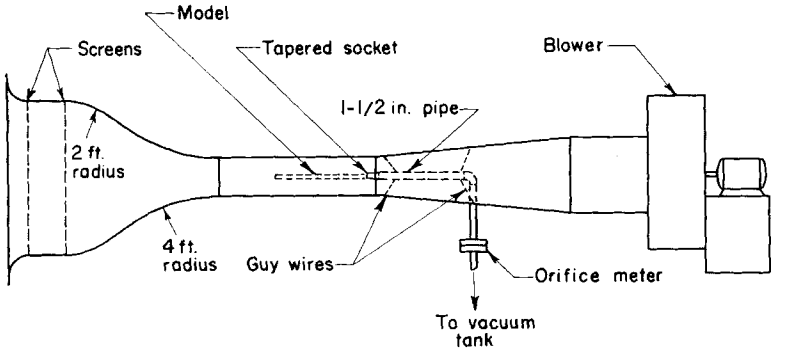

Fig. 3. Schematic of flow circuit.

controlled by proper adjustment of the velocity ratio R_u . Experimentally the value of R_u at which the transition occurs was found to be within the narrow range of 0.99 to 1.01.

To compare the test cylinders with the ideal model from the standpoint of uniformity of the velocity along the surface, pressure distributions over the outer surface were measured for various values of R_u . It was found that the pressure is essentially constant over the cylinder length for turbulent boundary layers, but that large velocity gradients occur near the leading edge (in the region of flow stagnation) for laminar boundary layers. However no influence of these gradients on the sublimation rate could be detected in sublimation experiments in which the velocity gradient was varied by altering R_u .

PRELIMINARY SUBLIMATION EXPERIMENTS

Verification of Profilometric Measurements

The small hemispherically-capped cylinder was used to check the profilometric technique gravimetrically. The total mass transfer rates obtained by the graphical integration of the measured local values were compared with direct weight-loss measurements. In every case the profilometric measurement was found to be within 2.8% of the gravimetric determination.

Effect of Velocity Ratio

Experiments with laminar boundary layers showed that variation of R_u from 1.01 to 1.25 caused no effect on the sublimation rates. The main sublimation experiments were performed in this range of R_u .

Effects of Yaw

The alignment of the models with the air stream was such that the yaw angle never exceeded 0.23 deg. The effect of such a small yaw on the mass transfer was shown to be negligible by direct sublimation experiments in which the angle of yaw was varied by 0.53 deg.

Disturbance Created at $x = x_{st}$

During sublimation a discontinuity at the juncture between the metal starting section and the subliming material was unavoidable. Experiments with laminar boundary layers established limits within which the sublimation rate was unaffected by changes in dimension of the subliming surface near its leading edge; these limits were observed in subsequent experiments.

In the turbulent-boundary-layer experiments a transient condition of the flow resulted from the gradually changing surface discontinuity at $x = x_{st}$ which caused mass transfer rates to vary continuously with time. This had to be taken into account in analyzing the turbulent-flow data.

RESULTS AND DISCUSSION

As it is usually defined, the mass-transfer coefficient is related to the local mass-transfer rate per unit area by the equation

$$\dot{m}'' = k_c \Delta c \qquad (4)$$

Since the relation of the local mass transfer rate to the rate of radius change is

$$\dot{m}'' = \rho_s(\Delta r/\Delta\tau) \qquad (5)$$

local mass transfer coefficients may be calculated from the profilometric data by the equation

$$k_c = (\rho_s/\Delta c)(\Delta r/\Delta\tau) \qquad (6)$$

In this instance the concentration difference of the vapor is virtually equal to the concentration at the surface (equilibrium concentration of the naphthalene for the prevailing temperature), since the free-stream concentration is immeasurably small. Consequently the concentration difference may be simply related to the vapor pressure of naphthalene by the ideal-gas law; that is,

$$\Delta c = c^* = p^* M/RT_s \qquad (7)$$

Correlations presented here are based on local coefficients of mass transfer calculated by using Equations (6) and (7) and on average coefficients obtained from the local values in accordance with

$$\bar{k}_c = (1/x)\int_0^x k_c\, dx \qquad (8)$$

The integral was obtained graphically from the laminar data; an empirical expression of k_c in terms of x was integrated analytically for the turbulent data.

Laminar Boundary Layer

Since the mass transfer coefficients are influenced by the presence of the metal starting section at the leading edge of the cylinder, allowance was made for this effect by analogy to the theoretical result of Bond (*24*) for the heat transfer through laminar boundary layers on a flat plate with unheated starting sections. According to Bond's analysis, if k_c is the measured mass-transfer coefficient and k_c' is the value of the coefficient that would exist at the same place if the starting section were replaced by subliming material, then the two are related as follows:

$$k_c' = k_c[1 - (x_{st}/x)^{\frac{3}{4}}]^{\frac{1}{3}} \qquad (9)$$

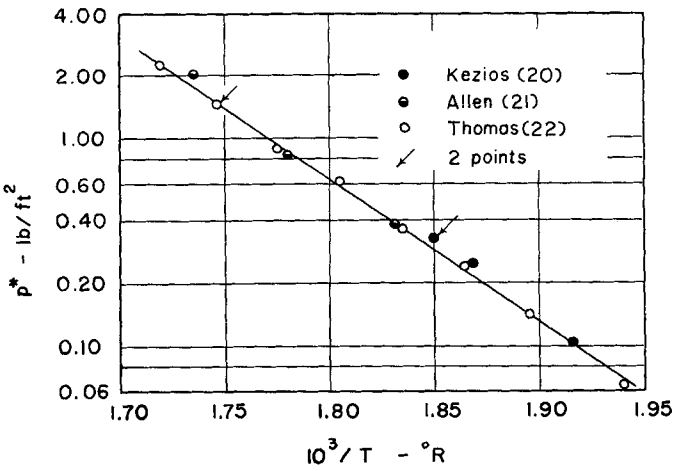

Fig. 4. Vapor pressure of naphthalene.

Any error introduced by this procedure is very small for distances from the leading edge greater than 1 in., where the magnitude of the correction is less than 7%.

Experimental results for the two cylinders with the highest range of air velocities employed (48 to 122 ft./sec.) have been correlated by the usual Sherwood-number*–Reynolds-number relationship†, as shown in Figure 6, since the effect of cylinder curvature is very small in this range of velocities. For the Reynolds number range of 4,000 to 100,000, where laminar boundary layers occurred, the data are represented by

$$N_{Sh}' = 0.454(N_{Re})^{\frac{1}{2}} \qquad (10)$$

$$\bar{N}_{Sh}' = 0.908(N_{Re})^{\frac{1}{2}} \qquad (11)$$

Maximum deviations of the data from Equations (10) and (11) are 8.0 and 3.5%, respectively, and average deviations are 2.5 and 1.6%, respectively.

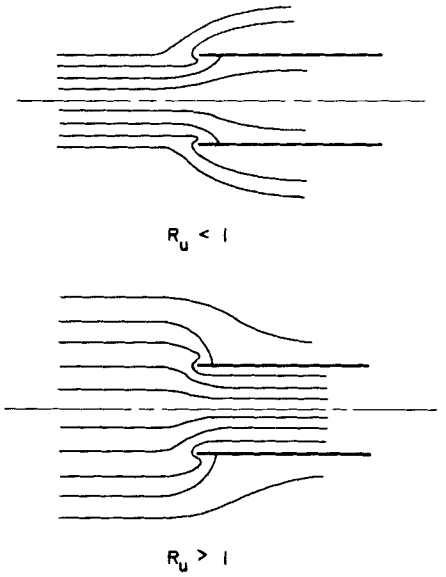

Fig. 5. Potential flow patterns for sharp-edged inlet.

For comparison of the results of Figure 6 with existing information on heat transfer and friction, it is convenient to use the Chilton-Colburn analogy, which is exact for the flat plate with small temperature and concentration differences. Reduced to the standard j-factor arrangement, Equations (10) and (11) take the form

$$j_M' = 0.339(N_{Re})^{-\frac{1}{2}} \qquad (12)$$

$$\bar{j}_M' = 0.678(N_{Re})^{-\frac{1}{2}} \qquad (13)$$

*Both Reynolds number N_{Re} and Sherwood number N_{Sh}' are based on total length x, the only characteristic length remaining after the condition $x_{st} = 0$ has been imposed.

†It has been suggested that this group $k_c x/\delta$, formerly referred to as the modified Nusselt number, be called the Colburn number. While there appears to be some justification for each of these designations, the name *Sherwood number* is employed here in conformance with the recently accepted chemical engineering terminology.

The results are thus shown to be 2.1% high compared with the Blasius equation for friction and the Pohlhausen relation for heat transfer. As shown later in the discussion of low-velocity experiments, this difference may be attributed to the effect of surface curvature on the mass transfer rate.

Previous investigations of heat and mass transfer from cylinders in axisymmetric flow have not utilized the sharp-edged model but rather cylinders with some sort of streamlined nose, and the results cannot be expected to agree with the present data. In fact the mass transfer data of Sogin and Jakob (*4*) for 0.37- and 1.3-in. naphthalene cylinders with inert hemispherical noses and the heat transfer data of Berman (*12*) for a 0.92-in. cylinder of ice with a rounded nose are generally lower than the present results at a Reynolds number of 10,000 and higher at Reynolds numbers near 100,000. Since these blunt leading edges may be expected to cause separation of the flow near the forward part of the cylinder and early transition of the boundary layer, the behavior of the results of Sogin and Jakob and of Berman can be logically attributed to the influence of the nosepieces. Their results might be expected to be low at small Reynolds numbers because of the predominant influence of the separated boundary layer, whereas the effect of early transition would cause the transfer rates to be unusually high at higher Reynolds numbers.

The heat transfer correlation reported by Jakob and Dow (*2*) for laminar flow over 1.3-in. cylinders with ellipsoidal and conical nosepieces is 2% lower than the present results and in excellent agreement with the exact solution of Pohlhausen for the flat plate. This agreement seems to be fortuitous however since Jakob and Dow made no allowance for the starting-length effect of their unheated nosepieces. If adjustment is made for the starting length according to Equation (9), their correlation falls about 6% below the Pohlhausen solution and 8% below the present results. A possible explanation for this discrepancy may be a separation of the boundary layer which extended over part of the heated cylinder.

The effect of transverse curvature on the mass transfer is demonstrated by the results for low air velocities (23 to 33 ft./sec.). The data are shown in Figure 7 in coordinates suggested by the results of previous theoretical treatments. These have invariably led to expressions of the following form:

$$(f/2)/(CN_{Re}^{-\frac{1}{2}}) = \psi_f(\xi) \qquad (14a)$$

$$j_H/(CN_{Re}^{-\frac{1}{2}}) = \psi_H(\xi) \qquad (14b)$$

$$j_M/(CN_{Re}^{-\frac{1}{2}}) = \psi_M(\xi) \qquad (14c)$$

In Equation (14) $\xi + (x/r)^2(N_{Re})^{-1}$ and C must equal 0.332 if the results are to agree with Blasius and Pohlhausen. Accordingly the mass transfer data (adjusted to zero starting length) are shown in the form $\psi_M = j_M'/(0.332N_{Re}^{-1/2})$ as a function of the variable ξ, along with curves representing the various theoretical results. The symbols used in Figure 7 are explained by Table 2.

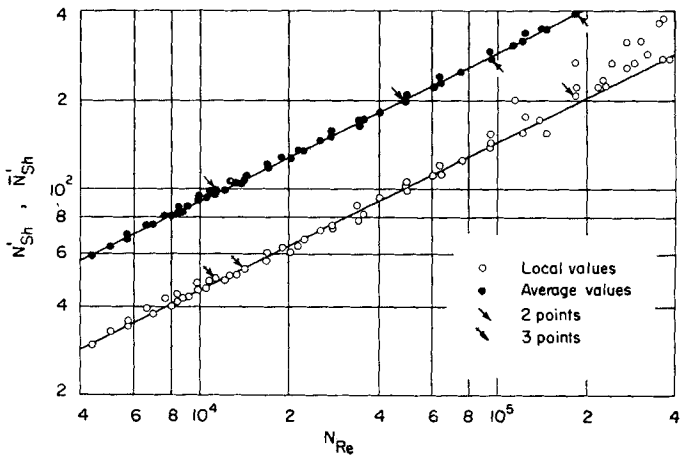

Fig. 6. Experimental results for mass transfer from sharp-edged cylinders with air velocities between 48 and 122 ft./sec.

Curve 1 in Figure 7, found originally by Young (*1*) for friction, was later obtained by Jakob and Dow (*2*) and applied to heat transfer by using the Reynolds analogy. Jakob and Dow evaluated the momentum integral through the boundary layer on a cylinder by using Pohlhausen's fourth-power polynomial for the velocity distribution and by assuming the boundary-layer thickness to be equal to that on a plane surface. Sogin and Jakob (*4*) performed a more elaborate analysis of the momentum boundary layer in obtaining curve 2 by using the same boundary-layer velocity profile without any assumption of the boundary-layer thickness; they applied

their results to mass transfer in accordance with the Chilton-Colburn analogy. The high value of C compared to the Blasius equation obtained by Young, by Jakob and Dow, and by Sogin and Jakob is apparently the result of the approximate velocity profile employed. Curve 3 was obtained by Seban and Bond (*3*), who numerically integrated the complete boundary-layer equations of energy and motion with $N_{Pr} = 0.715$, and it represents the only existing treatment of the effect of curvature on heat transfer which does not rely on some form of the analogy to friction. Seban and Bond also obtained results for friction that were later adjusted slightly by Kelly (*5*) (shown as curve 4). A solution for the friction on cylinders by Glauert and Lighthill (*8*), also represented by curve 3, is based on the momentum-integral approach with a logarithmic velocity profile in the boundary layer and results in a constant C which is 13% below the Blasius value. Curve 5 was obtained by Sowerby and Cooke (*6*), who used a modified Rayleigh analogy with the exact solution for the friction in the unsteady laminar flow over an impulsively started cylinder; the same result was found independently by Cooper and Tulin (*7*), who integrated linearized forms of the boundary-layer equations.

All of these analyses and the present work have neglected compressibility effects. Mention may be made that a theoretical treatment of the effect of transverse curvature on the skin friction in compressible flow has been given by Probstein and Elliot (*9*).

The experimental results are presented in Figure 7 by curve 6, which corresponds to the least-square correlation of the functional form suggested by the theoretical expressions, namely

$$\psi_M = 1 + 1.77\xi^{\frac{1}{2}} - 9.62\xi \qquad (15)$$

The maximum deviation of the data from Equation (15) is 6.7%, and the average deviation is 1.3%. Equation (15) may be written

$$j_M' = 0.332N_{Re}^{-\frac{1}{2}} \cdot (1 + 1.77\xi^{\frac{1}{2}} - 9.62\xi) \qquad (16)$$

This equation is based on data for N_{Re} between 12,000 and 100,000 and ξ between 0.0001 and 0.005.

On the basis of Equation (16) the discrepancy of 2.1% between Equation (12) and the Blasius and Pohlhausen expressions for flat surfaces may be attributed to surface curvature. Equation (16) indicates an increase of from 0.6 to 3.0% over the flat-plate values for the range of variables represented by Equation (12). The average increase of 1.8% is in good agreement with the actual difference of 2.1%.

Comparison of the present mass transfer results with the best solution for skin friction, represented by curve 4 in Figure 7, indicates that there is an effect of surface curvature on the analogy between skin friction and mass transfer amounting to about 6% at $\xi = 0.005$. Seban and Bond have already shown theoretically that such an effect occurs for the heat-transfer–friction analogy and have evaluated it for the specific case of $N_{Pr} = 0.715$. (Compare curves 3 and 4.) It is clear from their work that a corresponding effect of surface curvature on the mass-transfer–friction analogy must exist and that the magnitude of the effect is dependent on the Schmidt number (which is analogous to Prandtl number). This dependence is however not discernible solely on the basis of the differential equations of the boundary layer; exact comparison of the present experimental results with theory must await the solution of the system of nonlinear differential equations involved.

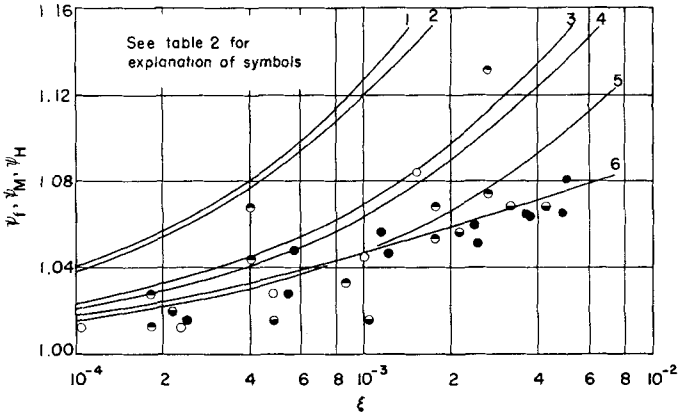

Fig. 7. Comparison of experiment values of ψ_M with theoretical results for the laminar boundary layer.

Turbulent Boundary Layer

Turbulent-boundary-layer experiments were performed at $R_u = 0.99$ and for $u_0 = 122$ ft./sec. by using both the 3/4- and 1-in. cylinders. Under operation at $R_u = 0.99$ the stagnation line falls on the inside of the nose of the cylinder, and therefore the production of turbulence is immediate at the leading edge.

The influence on the mass transfer of the transient discontinuity created at the end of the starting section had to be considered in the analysis of the data for turbulent boundary layers. While it is practically impossible to define accurately the geometry of such a discontinuity, its influence can be indexed in terms of the magnitude of the erosion Δr_i at a prescribed position just downstream. The position selected was about 1/16 in. behind the starting section. Mass transfer rates along the cylinder were obtained for various values

TABLE 2. SYMBOLS FOR FIGURE 7

Symbol or curve number	Explanation	Source
○	$u_0 = 32.6$ ft./sec., $D = 0.998$ in.	Present
◓	$u_0 = 32.9$ ft./sec., $D = 0.749$ in.	Present
●	$u_0 = 23.5$ ft./sec., $D = 0.749$ in.	Present
◒	$u_0 = 27.4$ ft./sec., $D = 0.749$ in.	Present
1	$\psi_H = \psi_f = 1 + 4\xi^{1/2}$; $C = 0.343$	(*1, 2*)
2	$\psi_M = \psi_f = \left[\frac{0.1762 + 0.153B/r}{6 - B/r}\right]^{1/2}\left[\frac{35.0}{6 - B/r}\right]^{*}$; $\xi = (B/r)^2\left[\frac{0.1762 + 0.153B/r}{6 - B/r}\right]^{1/2}$; $C = 0.343$	(*4*)
3	$\psi_H = 1 + 2.30\xi^{1/2} + \cdots$; $C = 0.332$	(*3*)
3	$\psi_f = 1 + 2.31\xi^{1/2} - 2.60\xi + \cdots$; $C = 0.289$	(*8*)
4	$\psi_f = 1 + 2.10\xi^{1/2} - 1.92\xi + \cdots$; $C = 0.332$	(*3, 5*)
5	$\psi_f = 1 + 1.50\xi^{1/2} - 0.722\xi + 1.09\xi^{3/2} + \cdots$; $C = 0.332$	(*6, 7*)
6	$\psi_M = 1 + 1.77\xi^{1/2} - 9.62\xi$; $C = 0.332$	Least-squares correlation of present results

*The symbol B denotes boundary-layer thickness.

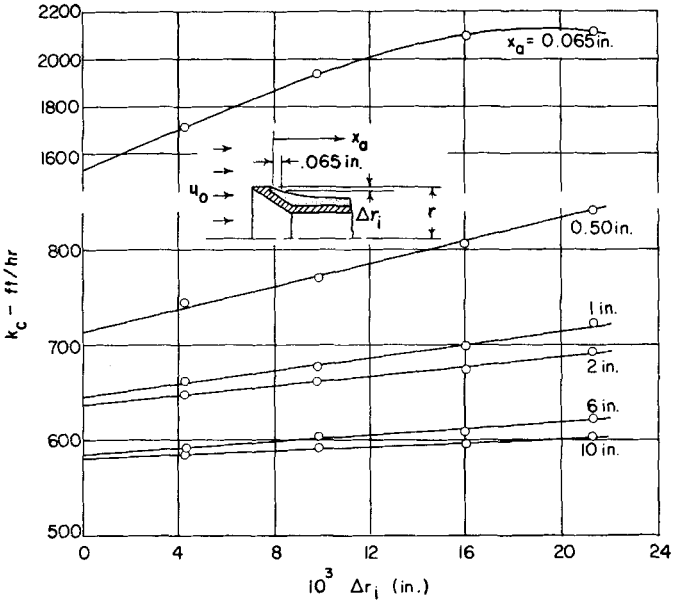

Fig. 8. Extrapolation of local mass transfer coefficients to zero-ridge conditions for induced-turbulence experiments.

of Δr_i from successive experiments with *identical operating conditions*. Then to obtain mass transfer coefficients uninfluenced by the discontinuity at $x = x_{st}$ the data were extrapolated to $\Delta r_i = 0$ (corresponding to time zero) when the naphthalene surface was continuous with the metal starting section. These extrapolated values of k_c were used in the correlations. Figure 8 is a typical plot of k_c vs. Δr_i for various axial positions along a cylinder.

The small starting-length effect of the metal nose of the cylinder was taken into account in accordance with an approximate procedure based on the empirical starting-length function defined by Tessin and Jakob (*14*) for turbulent boundary layers. If differentation of their expression is allowed, the relationship appropriate for adjusting the present data is*

$$k_c' = k_c[1 - x_{st}/x]^{0.09} \qquad (17)$$

As in the case of the laminar boundary layer, the magnitude of the adjustment obtained from Equation (17) is quite small, and the degree of accuracy achieved is sufficient, except near the leading edge.

The experimental results for both cylinders are presented in Figure 9; the range of Reynolds number covered is 10,000 to 1,000,000. Sherwood numbers employed there are based on values of the mass transfer coefficient reduced to zero starting length and to no surface discontinuity at the leading edge. In the Reynolds-number interval of 40,000 to 1,000,000 the data may be represented by a straight line having

$$N_{Sh}' = 0.00989(N_{Re})^{0.910} \qquad (18)$$

*That the exponent of 0.09 in Equation (17) remains unchanged in the differentiation is fortuitous; this occurs only when the exponent in Equation (18) is 0.910.

Table 3. Constant C and Exponent n of the Equation $\bar{N}_{Sh} = C(N_{Re})^n$ for Turbulent Boundary Layers According to Various Investigators

Source	Kind of work	Surface	C	n
(*26*)	Theo. (heat)	Plane	0.0178	0.876
(*28*)	Exp. (heat)	Plane	0.0330	0.849
(*27*)	Theo. (heat)	Plane	0.0245	0.876
(*29*)	Exp. (heat)	Plane	0.0226	0.876
(*2*)	Exp. (heat)	Cylinder	0.0196	0.876
(*31*)	Exp. (heat)	Plane	0.0226	0.876
(*32*)	Exp. (mass)	Plane	0.0273	0.872
(*33*)	Exp. (mass)	Plane	0.0624	0.792
(*14*)	Exp. (heat)	Cylinder	0.0216	0.876
Friction	Exp.	Plane	0.0342	0.837
Present work	Exp. (mass)	Cylinder	0.0109	0.910

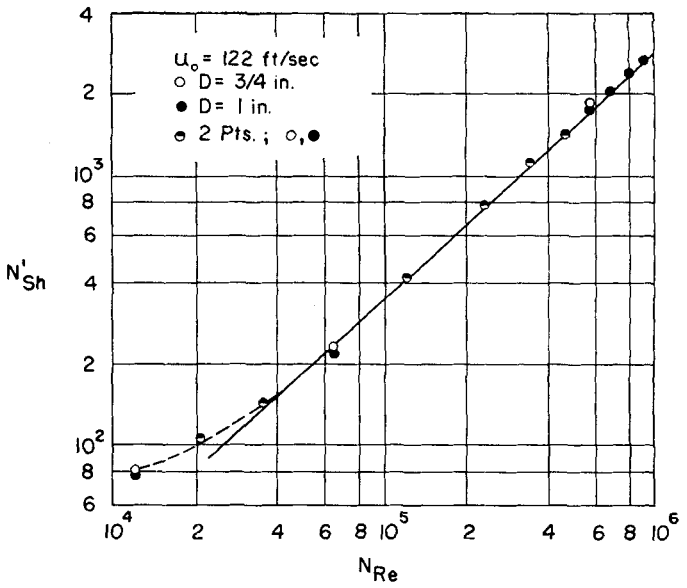

Fig. 9. Experimental results for local mass transfer from sharp-edged cylinders with artificially induced turbulence.

For comparison of the present data with the results of others it is convenient to use mean coefficients of mass transfer. The expression for the mean Sherwood number obtained by integration of Equation (18) is

$$\bar{N}_{Sh}' = 0.0109(N_{Re})^{0.910} \qquad (19)$$

It must be emphasized that Equation (19) is a form of the results which is suitable for comparison and as such is *not* an exact representation of the actual mean rates of mass transfer that occurred in the experiments, since Equation (18) does not hold over the entire cylinder length but fails in the vicinity of the leading edge, as can be seen from the data below $N_{Re} \cong 40{,}000$ in Figure 9 (dashed line). The reason for this behavior is not completely understood, but presumably it results from some sort of transitional flow near the leading edge or from invalidity of Equation (17) in that region.

Table 3 and Figure 10 compare the present results with those from a number of previous investigations. The comparisons have been made on the basis of the Boelter, Martinelli, and Jonassen (*25*) form of the heat-mass-momentum-transfer analogy, all results being transformed to Schmidt number $N_{Sc} = \nu/\delta = 2.40$. The power-function representations indicated in Table 3 are close approximations to the more complicated expressions obtained by means of the analogy.

Latzko's (*26*) theoretical work for

turbulent heat transfer along a flat plate is well-known; it is based on the von Kármán seventh-power law for velocity distribution and is carried out for a Prandtl number of unity. Seibert (*27*) obtained theoretical results for the flat plate with turbulent flow by employing a modification of Prandtl's momentum theory for Prandtl numbers other than unity, according to Jakob and Dow (*2*). Also, the experimental results of Juerges (*28*) and of Parmelee and Huebscher (*31*) were obtained with heated flat plates, none of which had a sharp leading edge. The correlation by Colburn (*29*) is based on the results of Juerges (*28*) and those of Elias (*30*), who used heated plates having sharp-edged, unheated nosepieces. The form presented here is based on the results obtained by Jakob and Dow (*2*) after correcting Colburn's original equation to zero starting length. Maisel and Sherwood (*32*) and Albertson (*33*), on the other hand, gathered data for the evaporation of water from flat plates. The friction results are those based on the well-known expression for skin friction on a flat surface, found by employing the Blasius expression for shear stress and the one-seventh-power velocity profile. Finally the heat transfer results of Jakob and Dow (*2*) and of Tessin and Jakob (*14*) were obtained by using cylinders having unheated nosepieces of various shapes and lengths.

The present results fall below all of the others shown in Figure 10, and they are in best agreement with the theoretical work of Latzko, being 14% below Latzko's value at $N_{Re} = 40{,}000$ but only about 2% lower at $N_{Re} = 1{,}000{,}000$. Comparison of results obtained on cylinders only shows that transfer rates for the sharp-edged cylinder are about 13% lower than those of Jakob and Dow and about 25% lower than those of Tessin and Jakob. This is not surprising in view of the disturbing influence of the nosepieces employed in both those investigations.

Though several approaches to the solution of laminar-boundary layers on cylinders in axial flow have been possible, one of which is apparently capable of producing exact results (*3*), treatment of the turbulent boundary layer has been limited to essentially one approach, based on assumptions that may not be valid. The procedure consists in evaluating the skin friction by a momentum integral with the one-seventh-power law of von Kármán assumed for the velocity profile of the boundary layer. Jakob and Dow (*2*) assumed in addition that the boundary-layer thickness on a cylinder is the same as on a plane surface and arrived at

$$\bar{f}/\bar{f}_p = 1 + 0.1125(N_{Re})^{-1/5}(x/r) \quad (20)$$

Landweber (*10*), Eckert (*11*), and Sogin and Jakob (*4*) all performed essentially the same analysis by assuming the flat-plate relation for skin friction in terms of boundary-layer thickness to be valid for the cylinder but with no restriction on the boundary-layer thickness. The results of these analyses is expressed by

$$\bar{f}/\bar{f}_p = \frac{2.41 + 0.723B/r}{(3 + B/r)^{4/5}} \quad (21)$$

$$(x/r)^{5/4}(N_{Re})^{-\frac{1}{4}} = 1.137(B/r)^{5/4}(3 + B/r) \quad (22)$$

Eckert's results, obtained for compressible flow, reduce to Equations (21) and (22) for Mach number zero.

The uncertainty of both of these solutions for $\bar{f}/\bar{f}_p$ is suggested by the results for laminar flow presented in Figure 7. It will be noted from comparison of curves 1 and 4 in that figure that the assumption of a fourth-power polynomial for the velocity profile of the boundary layer results in an error of about 10% in ψ_f when $\xi = 0.002$. A similar sensitivity of the solution to the assumed velocity profile may be inferred for the turbulent boundary layer also, and Eckert (*11*) has argued convincingly that such is the case. Furthermore Chapman and Kester (*15*) have demonstrated that there is a significant difference between the velocity profile of the turbulent boundary layer on a 1-in. cone cylinder and on a flat plate at $N_{Re} =$ 6,000,000 for supersonic flow. They also found an increase in the mean drag coefficient for subsonic flow over the cone cylinder amounting to 4%, as x/r increased from 16 to 46. For the same flow conditions, Equation (20) predicts an increase of 15%, and Equations (21) and (22) predict an increase of 1.5%; this fact suggests that the true solution for $\bar{f}/\bar{f}_p$ is intermediate to the existing theories but closer to Equations (21) and (22).

The present experimental results for turbulent boundary layers are unfortunately not sufficient to evaluate conclusively the effects of surface curvature on the mass transfer, since there seem to be no appropriate flat-plate values with which to compare. However the almost exact correspondence between data for the two cylinders (see Figure 9) suggests that the curvature effect is not large, thus favoring the result obtained by Landweber, by Eckert, and by Sogin and Jakob [Equations (21) and (22)]. At $N_{Re} = 600{,}000$ Equation (20) indicates a difference of over 10% between the local friction factors for the two cylinders employed here, whereas Equations (21) and (22) predict a difference of less than 1%. [Calculations by Sogin and Jakob (*4*) using the Boelter, Martinelli, and Jonassen (*25*) analogy indicate that the effect of curvature on the mass transfer with $N_{Sc} = 2.40$ is not significantly different from the effect of curvature on friction.]

The present results therefore lend some further confirmation to the result of Chapman and Kester (*15*), that the true effect of surface curvature on the turbulent boundary layer is close to that predicted by Equations (21) and (22). This being the case, mean coefficients of friction and heat or mass transfer should not exceed flat-plate values by more than 5% up to $(x/r)^{5/4}(N_{Re})^{-1/4} = 10$, as stated by Sogin and Jakob (*4*). Since this condition is not likely to occur* in practical situations, it seems safe to assume that no effect of transverse curvature exists in most instances where turbulent boundary layers occur.

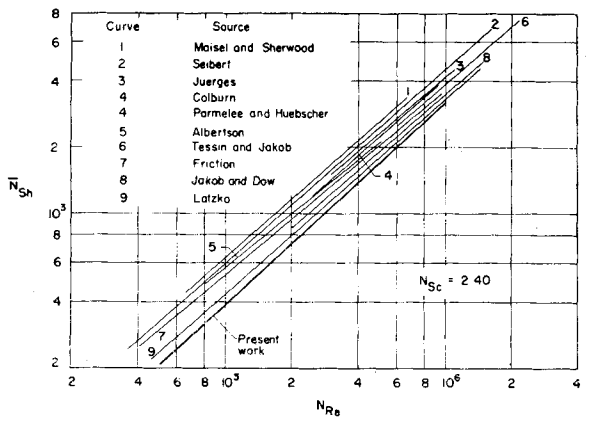

Fig. 10. Comparison of present experimental results with results of other investigators, turbulent boundary layers.

CONCLUSIONS

1. Local mass transfer coefficients for subliming cylindrical surfaces made of naphthalene can be precisely determined by mechanical profilometry.
2. It is possible to eliminate boundary-layer separation and premature transition associated with the use of solid nosepieces on cylinders in axisymmetric flow by employing sharp-edged hollow cylinders with internal suction.
3. By proper adjustment of the internal flow of a sharp-edged hollow cylinder, stable laminar boundary layers can be obtained on the external surface up to

*For air flow at 100 ft./sec. over a 1-in. cylinder the value of $(x/r)^{5/4}(N_{Re})^{-1/4}$ will exceed 10 only when the cylinder is over 5 ft. long.

Reynolds numbers of at least 100,000 (based on axial length). Also transition to turbulent boundary layer can be made to occur at the leading edge.

4. From the viewpoint of external flow the hollow cylinders employed closely simulate the idealized model, which has walls of zero thickness and uniform free-stream velocity along its length.

5. Local mass transfer rates through laminar boundary layers on the external surfaces of the test cylinders were found to be somewhat larger than corresponding flat-plate values because of transverse curvature. Also an effect of transverse curvature on the Chilton-Colburn analogy between momentum and mass transfer is indicated.

6. No influence of transverse curvature on the mass transfer through turbulent boundary layers was evident from the limited data obtained.

7. With allowance for the effect of curvature, the experimental results for laminar boundary layer are in excellent agreement with the theoretical predictions of Blasius and Pohlhausen for flat surfaces.

8. Based on the Boelter, Martinelli, and Jonassen analogy, the experimental results for turbulent boundary layers are in good agreement with Latzko's theoretical prediction for heat transfer from flat surfaces.

ACKNOWLEDGMENT

The paper is based partly on a thesis submitted in partial fulfillment of the requirements for the degree of Doctor of Philosophy at the Illinois Institute of Technology.

The authors are grateful for the support given to this investigation by the Office of Ordnance Research, United States Army, and for the cooperation in the early stages of the investigation of Alexander Sinila and H. H. Sogin.

NOTATION

B = boundary-layer thickness, ft.

$c(\Delta c)$ = concentration (concentration difference) of diffusing vapor, lb./cu. ft.

c^* = equilibrium concentration of naphthalene vapor for prevailing temperature, lb./cu. ft.

C = constant

D = diameter, ft.

f = local friction factor

$\bar{f}/\bar{f}_p$ = ratio of mean friction factor on a cylinder to that on a flat surface at equal Reynolds number

g = gravitational constant

j_M, $\bar{j}_M$ = local and average mass-transfer factors, respectively, $(k_c/u_0)(N_{Sc})^{2/3}$, $(\bar{k}_c/u_0)\ (N_{Sc})^{2/3}$

k_c, $\bar{k}_c$ = local and average mass transfer coefficients for air film, respectively, ft./hr.

$\dot{m}''$ = local mass-transfer rate, lb./sq. ft.

M = molecular weight of naphthalene

N_{Pr} = Prandtl number, ν/α

N_{Re} = Reynolds number, u_0x/ν

N_{Sc} = Schmidt number, ν/δ

N_{Sh}, $\bar{N}_{Sh}$ = local and average Sherwood numbers, respectively, k_cx/δ, $\bar{k}_cx/\delta$

p = pressure, lb./sq. ft.

p^* = vapor pressure of solid naphthalene, lb./sq. ft.

$r(\Delta r)$ = radius (radius change) of cylinder, in., ft.

R = universal gas constant, ft.-lb./(lb.-mole)(°R.)

R_u = ratio of velocity at cylinder inlet to free-stream approach velocity (uniform distribution of internal flow over cylinder inlet assumed)

t, T = temperature. °F. and °R. respectively

u = air velocity, ft./sec., ft./hr.

x = axial distance from leading edge, in., ft.

α = thermal diffusivity, sq. ft./hr.

δ = mechanical diffusivity, sq. ft./hr.

ν = kinematic viscosity, sq. ft./hr.

ξ = $(x/r)^2(N_{Re})^{-1}$

ρ = density, lb./cu. ft.

ρ_0 = air density

$\Delta\tau$ = time increment, hr.

$\psi(\xi)$ = function defined by Equation (14) and represents ratio of transfer from curved surface to transfer from flat plate

Subscripts

a = active (subliming) length

1 = local condition at outer edge of boundary layer

M = mass transfer

f = friction

H = heat transfer

0 = free-stream approach condition

s = surface or solid

st = starting length

Superscripts

' (prime) = adjusted to zero starting length

LITERATURE CITED

1. Young, A. D., *Aeronaut. Research Council (Great Britain) Rept. Mem.* 1874 (1939).
2. Jakob, Max, and W. M. Dow, *Trans. Am. Soc. Mech. Engrs.*, **68**, 123 (1945).
3. Seban, R. A., and R. Bond, *J. Aeronaut. Sci.*, **18**, 671 (1951).
4. Sogin, H. H., and Max Jakob, *Heat Transfer and Fluid Mech. Inst., Preprints*, p. 5, Univ. Southern Calif., Los Angeles, California (1953).
5. Kelly, H. R., *J. Aeronaut. Sci.*, **21**, 634 (1954).
6. Sowerby, L., and J. C. Cooke, *Quart. J. Mech. and Appl. Math.*, **6**, 50 (1953).
7. Cooper, R. D., and M. P. Tulin, *David W. Taylor Model Basin, Rept.* 838 (1953).
8. Glauert, M. B., and M. J. Lighthill, *Proc. Roy. Soc. (London)*, **A230**, 188 (1955).
9. Probstein, R. F., and David Elliot, *J. Aeronaut. Sci.*, **23**, 208, 236 (1956).
10. Landweber, L., *David W. Taylor Model Basin, Rept.* 689 (1949).
11. Eckert, H. U., *J. Aeronaut. Sci.*, **19**, 23 (1952).
12. Berman, Kurt, *Trans. Am. Soc. Mech. Engrs.*, **76**, 397 (1954).
13. Powell, R. W., *Trans. Inst. Chem. Engrs. (London)*, **18**, 26 (1940).
14. Tessin, William, and Max Jakob, *Trans. Am. Soc. Mech. Engrs.*, **75**, 473 (1953).
15. Chapman, D. R., and R. H. Kester, *Natl. Advisory Comm. Aeronaut., Tech. Note* 3097 (1954).
16. Jakob, Max, and G. A. Hawkins, "Elements of Heat Transfer and Insulation," John Wiley, New York (1942).
17. Eucken, Arnold, and Max Jakob, ed., "Der Chemie Ingenieur," vol. I, part 1, pp. 69–73, Akademische Verlagsgesellschaft M.B.H., Leipzig (1933).
18. Gilliland, E. R., *Ind. Eng. Chem.*, **26**, 681 (1934).
19. "International Critical Tables," vol. I, p. 233, McGraw-Hill, New York (1926).
20. Jakob, Max, S. P. Kezios, Alexander Sinila, H. H. Sogin, and Maurice Spielman, *U. S. Air Force, Tech. Rept.* 6120, Part 5, Illinois Inst. Tech., Chicago (1952).
21. Allen, R. W., *J. Chem. Soc. (London)*, **77**, 400 (1900).
22. Thomas, J. H. G., *J. Soc. Chem. Ind. (London)*, **35**, 506 (1916).
23. Fradenburgh, E. A., and D. D. Wyatt, *Natl. Advisory Comm. Aeronaut., Tech. Note* 3004 (1953).
24. Bond, R., *Inst. Eng. Research*, Univ. California, Berkeley (March, 1950).
25. Boelter, L. M. K., R. C. Martinelli, and Finn Jonassen, *Trans. Am. Soc. Mech. Engrs.*, **63**, 447 (1941).
26. Latzko, H., *Z. angew. Math. u. Mech.*, **1**, 268 (1921); transl.: *Natl. Advisory Comm. Aeronaut., Tech. Mem.* 1068 (1944).
27. Seibert, Otto, *Jahrb.* 1938 *deut. Luftfahrforsch.*; transl.: *Natl. Advisory Comm. Aeronaut., Tech. Mem.* 1044 (1943).
28. Juerges, W., *Beih. Gesundh. Ingr.*, Reihe 1, Beih. 19, Munich and Berlin (1924).
29. Colburn, A. P., *Trans. Am. Inst. Chem. Engrs.*, **29**, 174 (1933).
30. Eliás, Franz, *Z. angew. Math. u. Mech.*, **9**, 433 (1929); **10**, 1 (1930); transl.: *Natl. Advisory Comm. Aeronaut., Tech. Mem.* 614 (1931).
31. Parmelee, G. V., and R. G. Huebscher, *Trans. Am. Soc. Heating and Ventilating Engrs.*, **53**, 245 (1947).
32. Maisel, D. S., and T. K. Sherwood, *Chem. Engr. Progr.*, **46**, 131 (1950).
33. Albertson, M. L., *Heat Transfer and Fluid Mech. Inst., Preprints*, 243, Stanford Univ., Stanford, Calif. (1951).

Manuscript received September 5, 1957; revision received May 5, 1958; paper accepted May 23, 1958. Paper presented at A.I.Ch.E. Baltimore meeting.